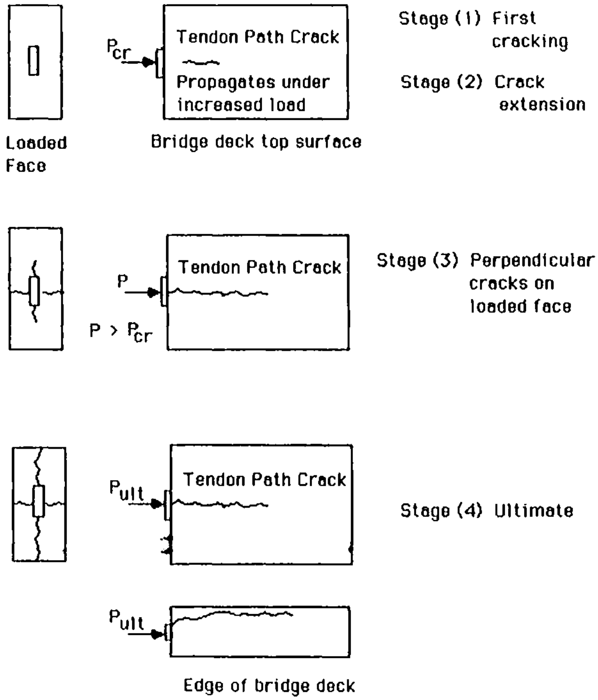

Fig. 7--Failure sequence for single monostrand anchorage specimens

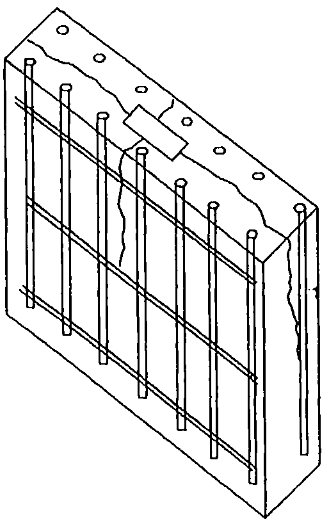

Fig. 8--Crack pattern of single monostrand anchorage specimens superimposed with bridge deck reinforcement

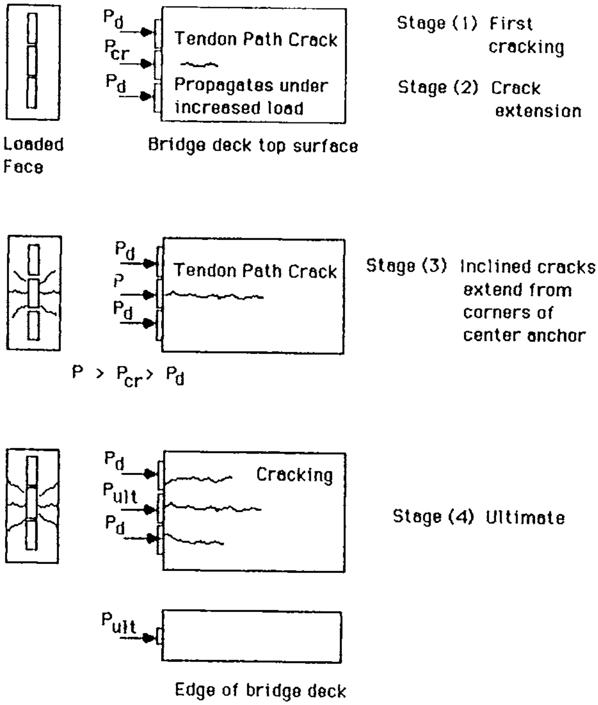

Fig. 9--Failure sequence for closely-spaced monostrand anchorage specimens

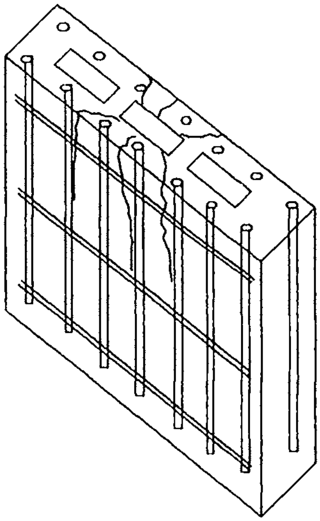

Fig. 10--Crack pattern of closely-spaced monostrand anchorage specimens superimposed with bridge deck reinforcement

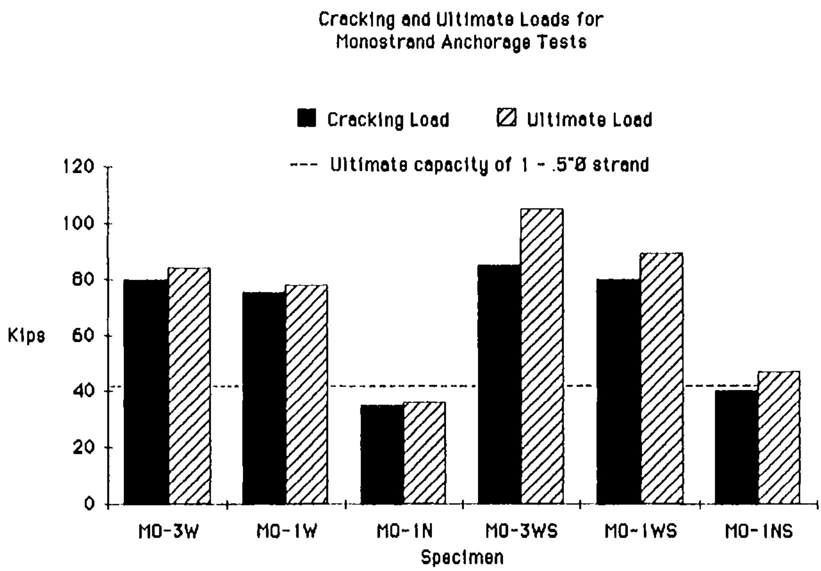

Fig. 11--Monostrand anchor series test results

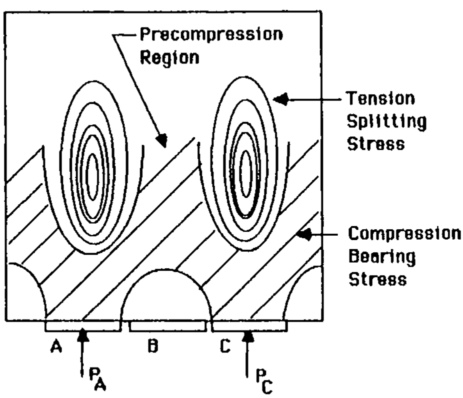

Fig. 12--Precompression of center anchorage zone during stressing of outer anchorages

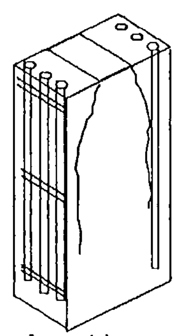

Fig. 13--Crack pattern of the narrow, single monostrand anchorage specimens superimposed with bridge deck reinforcement

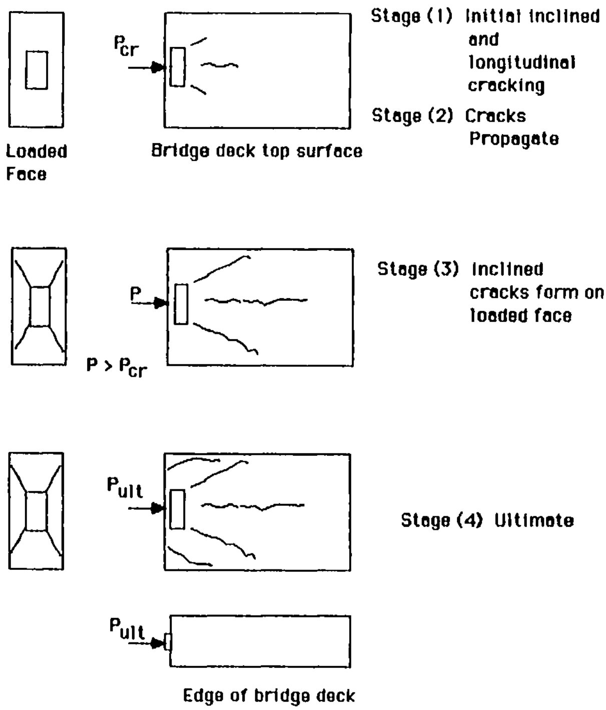

Fig. 14--Failure sequence for single and closely-spaced multistrand anchorage specimens

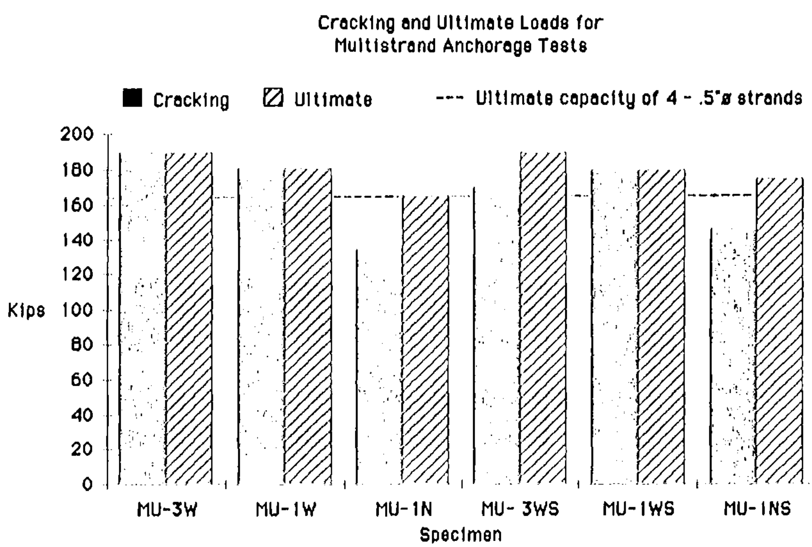

Fig. 15--Multistrand anchor series test results

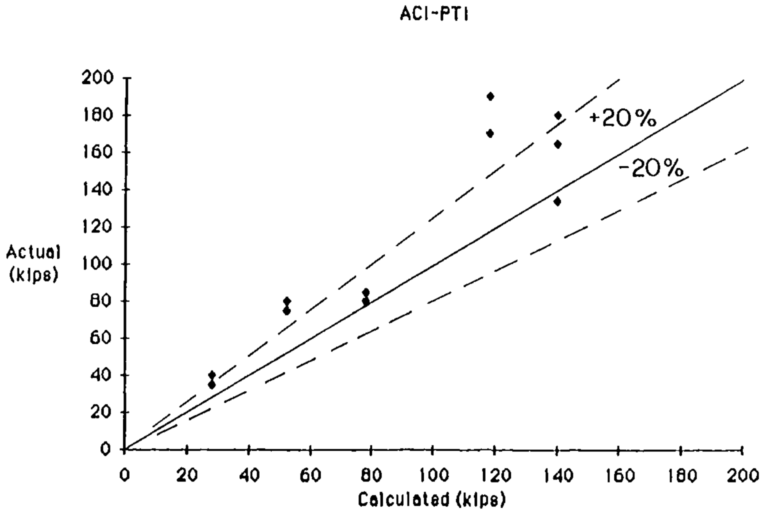

Fig. 16--ACI-PTI calculated cracking load versus actual cracking load

TABLE 10--ACI-PTI CALCULATED VERSUS ACTUAL CRACKING LOAD

Specimen	Calculated Cracking Load	Actual Cracking Load	P_{act}/P_{cal}
MO-1N	28	35	1.25
MO-1NS	28	40	1.43
MO-1W	52	75	1.44
MO-1WS	52	80	1.54
MO-3W	78	80	1.03
MO-3WS	78	85	1.09
MU-1N	140	134	0.96
MU-1NS	140	165	1.18
MU-1W	140	181	1.29
MU-1WS	140	180	1.29
MU-3W	118	190	1.61
MU-3WS	118	170	1.44

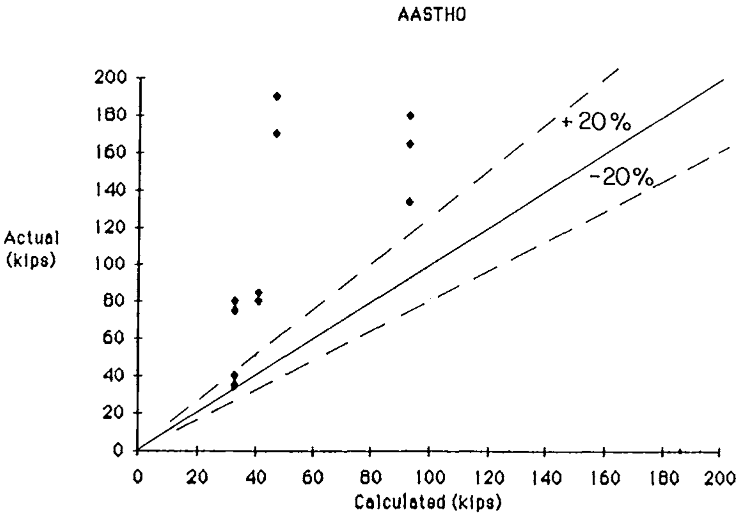

Fig. 17--AASHTO calculated cracking load versus actual cracking load

TABLE 11--AASHTO CALCULATED VERSUS ACTUAL CRACKING LOAD

Specimen	Calculated Cracking Load	Actual Cracking Load	P_{act}/P_{cal}
MO-1N	33	35	1.06
MO-1NS	33	40	1.21
MO-1W	33	75	2.27
MO-1WS	33	80	2.42
MO-3W	41	80	1.95
MO-3WS	41	85	2.07
MU-1N	93	134	1.44
MU-1NS	93	165	1.77
MU-1W	93	181	1.95
MU-1WS	93	180	1.94
MU-3W	47	190	4.04
MU-3WS	47	170	3.62

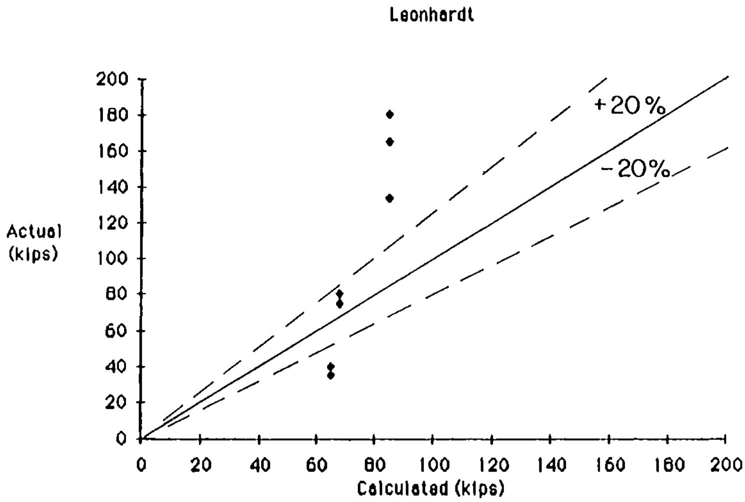

Fig. 18--Leonhardt's calculated cracking load versus actual cracking load

TABLE 12--LEONHARDT'S CALCULATED VERSUS ACTUAL CRACKING LOAD

Specimen	Calculated Cracking Load	Actual Cracking Load	P_{act}/P_{cal}
MO-1N	65	35	0.54
MO-1NS	65	40	0.62
MO-1W	68	75	1.10
MO-1WS	68	80	1.18
MU-1N	85	134	1.58
MU-1NS	85	165	1.94
MU-1W	85	181	2.13
MU-1WS	85	180	2.12

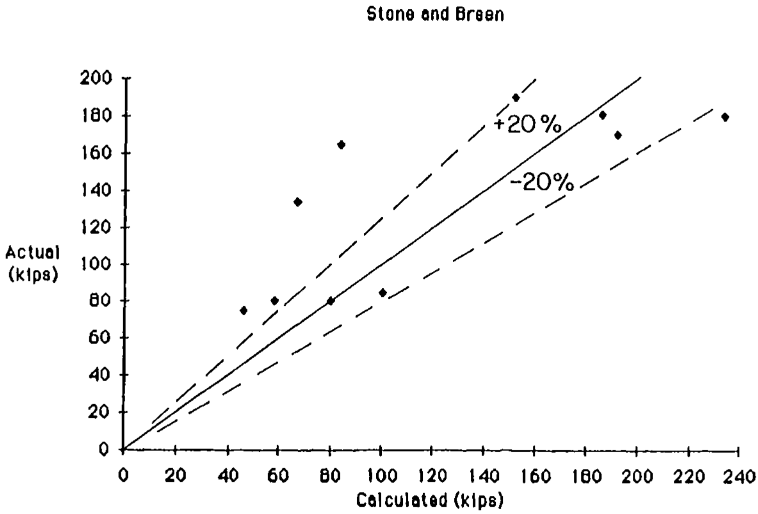

Fig. 19--Stone and Breen calculated cracking load versus actual cracking load

TABLE 13--STONE AND BREEN CALCULATED VERSUS ACTUAL CRACKING LOAD

Specimen	Calculated Cracking Load	Actual Cracking Load	P_{act}/P_{cal}
MO-1N	N.A.	35	N.A.
MO-1NS	N.A.	40	N.A.
MO-1W	46	75	1.63
MO-1WS	58	80	1.38
MO-3W	80	80	1.00
MO-3WS	101	85	0.84
MU-1N	67	134	2.00
MU-1NS	84	165	1.96
MU-1W	180	181	1.01
MU-1WS	234	180	0.77
MU-3W	152	190	1.25
MU-3WS	192	170	0.89

SP 113-5

Stresses, Strains, and Bursting Cracks in Anchorage Zones of Post-Tensioned Beams

by E.G. Nawy

Synopsis: This paper discusses the stresses, strains, and the development of bursting cracks at the end block anchorage zones of post-tensioned prestressed concrete beams. It covers the two stages of loading, namely, the longitudinal prestressing loading stage and the additional transverse loading at the third span point applied during the beam testing stage. The effects of the transverse shear force on the stress/strain distributions and end block cracking of concentrically and eccentrically post-tensioned beams with rectangular anchorage blocks were studied. A three-dimensioanl embeddable strain gage tripod frame was developed and fabricated in this investigation to measure the interior strains in the anchorage blocks of fifteen beams subjected first to initial prestressing and subsequently to additional transverse shear loading. Surface concrete strains were also measured through the use of strain rosettes mounted on the concrete surface at critical locations in the anchor blocks. The measured strains were compared to the analytical strain curves and contours produced by a linear, isotropic, three-dimensional finite element model. The peak lateral bursting stress was found to be greater and located nearer to the bearing surface than the peak transverse bursting stress. The transverse external shear load was generally found to be reaching the peak transverse bursting strain but had little effect on the peak lateral bursting strain. The bursting cracks in the longitudinal direction across the beam lateral thickness as well as the spalling cracks result when the three-dimensional stresses exceed the modulus of rupture of concrete, but can be controlled through the use of adequate vertical reinforcement in the anchorage stress transition zone.

Keywords: anchorage (structural); beams (supports); cracking (fracturing); end blocks; finite element method; post-tensioning; prestressed concrete; reinforcing steels; strains; stresses

Edward G. Nawy, FACI, is Professor of Civil Engineering, Rutgers, The State University of New Jersey, holding the distinguished professor rank (Professor II). Active in ACI since 1949, Prof. Nawy is a former chairman and current member of ACI Committee 224, Cracking, and is currently a member of ACI Committee 340, Design Aids for ACI Building Codes, 435, Deflection of Concrete Building Structures; Joint ACI-ASCE Committee 421, Design of Reinforced Concrete Slabs; the Concrete Materials Research Council; Technical Activities Committee of PCI, and the Tall Buildings Council. His research interests are in reinforced and prestressed concrete, particularly in the areas of crack control and serviceability behavior. Prof. Nawy has published more than 100 papers and is the author of three major text-books: Reinforced Concrete - A Fundamental Approach, Simplified Reinforced Concrete, and Prestressed Concrete - A Fundamental Approach as well as numerous handbook chapters. He holds many honors and awards, including the ACI Chapter Activities Committee and Henry L. Kennedy Awards, was twice President of the N.J. ACI chapter, served two terms on the Rutgers University Board of Governers, was Honorary Vice President of the RILEM 30th Anniversary Congress, and is Honorary Professor of NIT, the Nanjing Institute of Technology. He is consultant to major organizations in the New York-New Jersey metropolitan area, and is a registered Professional Engineer in New Jersey, New York, and Pennsylvania.

INTRODUCTION

This paper deals with the distribution of stresses and strains at the rectangualr anchorage zones of post-tensioned prestressed beams subjected to transverse shear force and the longitudinal cracking in these zones. It describes the behavior of 15 beams prestressed with either concentric or eccentric prestressing tendons loaded transverely and tested to failure. The study of strains and stresses in the anchorage zone covers two stages of loading, namely, the inital post-tensioning stage and the subsequent transverse loading stage applied during the beam tests to failure.

In addition to measuring the concrete surface strains, embeddable three-dimensional strain gage steel tripod frames developed for this investigation were used to measure the internal longitudinal, lateral and transverse strains in the concrete. The longitudinal (x) direction is along the beam span while the transverse (y) and lateral (z) axes are respectively in the vertical and horizontal directions. The three-dimensional strain measurements within the concrete in the anchorage zone facilitated the interpretation of the stress conditions caused by prestressing and by transverse load resulting in the splitting and bursting cracks in these zones. Analysis and interpretation of the test results was facilitated by using a three-dimensional finite elements model named ANSYS Version 4.2 in this investigation.